
Forecasting Long-Term Trends of the COVID-19 Outbreak in Yazd with an SVIR Model

Mohammad Hossein Akrami¹, J. Ayatollahi², S.A. Mousavi²,
M. Sharifyazdi², Z. Akhondimeybodi², F. Heidari²

¹Department of Mathematical Science, Yazd University, Yazd, Iran

²Infectious Diseases Research Center, Shahid Sadoughi Hospital, Shahid Sadoughi
University of Medical Sciences, Yazd, Iran

ABSTRACT. This article examines the transmission of COVID-19 from a mathematical model perspective, analyzing its spread pattern. Given the virus's adherence to standard epidemic disease transmission principles and the effectiveness of vaccination in mitigating and controlling its spread, we employ the SVIR model to demonstrate the disease's progression in Yazd. The data used in this study was provided by the medical care monitoring center of Yazd Shahid Sadoughi University of Medical Sciences, Yazd, Iran, for 770 days between September 27, 2020 to November 5, 2022. To establish the parameters, we utilized the genetic algorithm (GA) to minimize the cost function between the model's prediction and the real data. Additionally, we conducted our simulations using Matlab software. Identifying the factors that contribute to the spread of the virus through mathematical modeling can be a crucial step towards controlling the disease, given its catastrophic impact on the economy, society, and health.

Keywords: Epidemic mode; SVIR; Public health; Pandemic; COVID-19.

2010 Mathematics subject classification: 34A08, 37N25; Secondary 34K20.

¹Corresponding author: akrami@yazd.ac.ir


Received: 08 May 2024

Revised: 28 July 2024

Accepted: 30 July 2024

How to Cite: Akrami, Mohammad Hossein; Ayatollahi, Jamshid; Seyed Alireza, Mousavi; Sharifyazdi, Mohammad; Akhondi Meybodi, Zohreh; Heydari, Faezeh. Forecasting Long-Term Trends of the COVID-19 Outbreak in Yazd with an SVIR Model, *Casp.J. Math. Sci.*, **13**(2)(2024), 296-310.

This work is licensed under a Creative Commons Attribution 4.0 International License.

 Copyright © 2024 by University of Mazandaran. Submitted for possible open access publication under the terms and conditions of the Creative Commons Attribution(CC BY) license(<https://creativecommons.org/licenses/by/4.0/>)

1. INTRODUCTION

The COVID-19, an abbreviation for Coronavirus Disease 2019, is an exceptionally transmissible respiratory sickness instigated by the newly discovered coronavirus, SARS-CoV-2. It emerged initially in December 2019 in Wuhan, China [12, 19, 20, 21]. It rapidly spread globally, leading to a pandemic. Iran reported its first confirmed cases of COVID-19 on February 19, 2020 [1]. The source of the initial infections in Iran is believed to be from individuals who had traveled to affected areas or had direct contact with infected individuals. In response to the growing COVID-19 threat, Iran swiftly implemented various quarantine measures to contain the spread of the virus. On February 27, 2020, the Iranian government imposed nationwide lockdowns, restricted travel, and closed schools, universities, and religious sites. These measures aimed to limit social interactions, enforce physical distancing, and promote personal hygiene practices [2, 14]. Additionally, Iran established screening checkpoints at airports and borders, implemented contact tracing protocols, and conducted extensive testing to identify and isolate infected individuals promptly. These measures were vital in controlling the transmission of the virus and reducing the burden on healthcare systems.

Yazd City, located in central Iran, reported its first case of COVID-19 on March 2020. As it is situated at the center of Iran, this area serves as the primary route for travelers to access other regions, making it a crucial factor in the spread of Covid-19. [10]. Following the initial report, health authorities in Yazd City swiftly initiated a series of comprehensive measures to address the situation. In response to the COVID-19 outbreak, local authorities in Yazd City implemented stringent quarantine measures to limit the spread of the virus. These measures included the closure of non-essential businesses, schools, and public spaces. Travel restrictions were also imposed to prevent further transmission within and outside the city. The authorities worked closely with healthcare professionals to conduct extensive testing, contact tracing, and isolation of confirmed cases to curb the outbreak's progression. In addition to quarantine measures, public health campaigns were launched to raise awareness about COVID-19 symptoms, prevention strategies, and the importance of hygiene practices such as handwashing and mask-wearing.

To understand the dynamics and spread of the coronavirus, scientists and researchers turned to mathematical modeling, for example see [3, 4, 11, 17, 22] and references therein. Developed in the early 20th century, the SIR model represented a breakthrough in understanding the spread of infectious diseases by dividing the population into three distinct compartments [6, 9, 15]. Although short-term prediction of disease was anticipated by the SIR model, this model could not accurately predict the long-term spread and pattern of the epidemic. Interestingly, many SIR models published for other communities to forecast COVID-19 also faced similar discrepancies [13]. Therefore, for a more accurate estimate, a model with more assumptions is needed. On the other hand, vaccination is considered an effective strategy to prevent COVID-19 and control the spread of the disease [5]. Hence, SVIR model provides

valuable insights into the transmission and progression of infectious diseases like COVID-19.

In this paper, we consider an SVIR model to fit the COVID-19 data from Yazd city. Given that these types of models are unimodal, we divide the time period into five intervals. Each interval contains a single peak, and by fitting the model to the data of each interval, we estimate the model parameters using a genetic algorithm. To utilize the genetic algorithm, we need to define a cost function, which we consider as the sum of the squared errors between the real data and the number of infectious individuals obtained from the model. We then solve the system using numerical methods for solving differential equations. Numerical simulations are performed using the ode45 in MATLAB. The results are then compared and validated against real-world data from Yazd city in Iran. The ode45 function in MATLAB is based on an adaptive step size Runge-Kutta method known as the Dormand-Prince method. The Dormand-Prince method uses a fifth-order method to estimate the error and a fourth-order method for the solution. This allows the solver to adjust the step size dynamically to achieve a specified accuracy [16].

The rest of the paper is organized as follows: Section 2 introduces the model and investigates the existence, uniqueness, and positivity of the solutions. Additionally, we analyze the stability of the equilibrium points. In Section 3, we examine the data and fit the model accordingly, estimating the model parameters and their confidence intervals for each of the five time periods. The paper ends with the Conclusion section.

2. THE MODEL

Although the classic SIR model is a simplistic compartmental model that can describe the spread of a virus in a community, it fails to account for the impact of a vaccinated population on the dynamics of susceptible (S), infected (I), and removed (R) individuals. In this study, we aim to investigate the spread of a virus, such as COVID-19, and its relationship with varying levels of vaccination across interconnected communities. To achieve this, we adopt the susceptible-vaccinated-infected-removed (SVIR) model introduced by Tornatore et al. in [18]:

$$\begin{aligned}\frac{dS}{dt} &= \eta - \alpha SI - (\eta + \sigma)S, \\ \frac{dV}{dt} &= \sigma S - \vartheta \alpha IV - \eta V, \\ \frac{dI}{dt} &= \alpha SI + \vartheta \alpha IV - (\lambda + \eta)I, \\ \frac{dR}{dt} &= \lambda I - \eta R.\end{aligned}\tag{2.1}$$

The SVIR model (2.1) is based on the classic SIR model but includes modifications to account for vaccination programs. Specifically, the model considers the impact of a vaccine that does not lose its efficacy over time and assumes that a fraction σ of

the susceptible population, S , is vaccinated in each unit of time. The vaccination may reduce but not eliminate susceptibility to infection, so the model includes a factor ϑ , where $0 \leq \vartheta \leq 1$, in the contact rate of vaccinated individuals, V , with $\vartheta = 0$ corresponding to perfect vaccine efficacy and $\vartheta = 1$ to no effect. Parameter λ is the rate of recovered individuals in the community, η is the birth and death rate, and α is the transmission rate of susceptible to infected individuals.

The model also assumes permanent immunity, such that a fraction λ of infected individuals, I , returns to the removed population, R . Additionally, the model considers constant rates of births and deaths, with all newborns entering the susceptible population, S . Therefore, all parameters in the model, including η , λ , σ , and α , are positive real numbers.

Motivated by the work in [4, 18], we introduce the following system of coupled ODEs:

$$\begin{aligned}\frac{dS}{dt} &= -\alpha SI - \sigma S, \\ \frac{dV}{dt} &= \sigma S - \vartheta \alpha IV, \\ \frac{dI}{dt} &= \alpha SI + \vartheta \alpha IV - \lambda I, \\ \frac{dR}{dt} &= \lambda I.\end{aligned}\tag{2.2}$$

This model is based on several key assumptions:

- The population is homogeneous and only a single disease is spreading among them.
- All parameters, including the transmission rate from susceptible to infected individuals (α), vaccine efficacy parameters (ϑ), the fraction of the susceptible population that is vaccinated (σ), and the recovery rate (λ), are positive.
- The rate at which new susceptible individuals join the population (through births or migration) is equal to the rate at which individuals leave the population (through deaths or migration), so these rates are not included in the model.
- Given that the vaccine does not provide complete immunity, a percentage of vaccinated individuals may still become infected and fall ill when exposed to the disease.

The SVIR model incorporates a vaccinated compartment, which is crucial for accurately modeling the impact of COVID-19 vaccination campaigns on the spread of the virus. This is particularly relevant for Yazd city, where significant vaccination efforts were undertaken during the study period. By dividing the population into four distinct compartments—susceptible, vaccinated, infected, and recovered—the SVIR model allows for a detailed analysis of how different segments contribute to the epidemic.

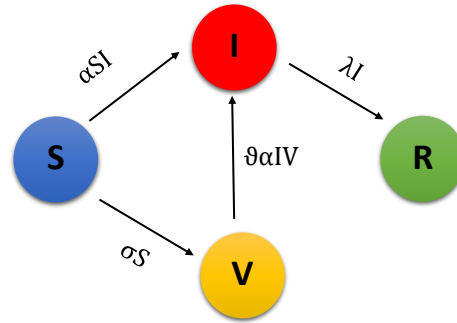


FIGURE 1. Schematic flow diagram of the SVIR model.

The flexibility of the SVIR model enables it to be adapted to various epidemic scenarios by adjusting parameters, making it suitable for the dynamic nature of the COVID-19 pandemic. This adaptability is crucial for reflecting local conditions, vaccination rates, and other factors specific to Yazd city. Additionally, the model is well-suited to the available infection data, allowing for effective parameter estimation and validation. The robustness and predictive power of the SVIR model make it a reliable tool for forecasting the epidemic's future course and assessing the impact of public health interventions, which is critical for informing policy decisions in Yazd city. The system of equations (2.2) is obtained by modifying the original single SVIR model (2.1) with the assumption that there are no births or deaths in the community except for those caused by the virus, similar to the classic SIR model. This is achieved by setting $\eta = 0$. It is important to note that in the modified model (2.2), the sum of susceptible, vaccinated, infected, and removed individuals is always equal to the total population, denoted by N , which remains constant over time. Therefore, the SVIR model provides a more realistic representation of virus spread in a vaccinated population than the classic SIR model. The population-flux diagram in Fig. 1 illustrates how the four populations in the system of equations (2.2) interact with each other within a community, representing the transfer of individuals between susceptible, vaccinated, infected, and removed groups.

2.1. Existence, uniqueness and boundedness of solutions. This subsection examines the analytical properties of solutions for our proposed epidemic model. The solution must be nonnegative and bounded. We will explore these characteristics below.

First, we define

$$\Gamma = \{(S, V, I, R) \in \mathbb{R}^4 : S \geq 0, V \geq 0, I \geq 0, R \geq 0, S + V + I + R = 1\}.$$

In the following, we prove that the solution remains in Γ .

Theorem 2.1. (Theorem 2.1, [18]) *If $(S(0)V(0), I(0), R(0)) \in \Gamma$, then there exists $T > 0$ and a unique solution $(S(t), I(t), V(t), R(t))$ to the system (2.1) on $t \in [0, T)$ almost surely.*

Now, Theorem 2.1 implies following theorem about boundedness of solution in Γ .

Theorem 2.2. *Suppose $(S(t), I(t), V(t), R(t))$ be a solution of system (2.1) on $[0, T)$. If $S(\tau) > 0, V(\tau) > 0, I(\tau) > 0, R(\tau) > 0$, for all $\tau \in [0, T)$, then*

$$0 < S(\tau) < 1, \quad 0 < V(\tau) < 1, \quad 0 < I(\tau) < 1, \quad 0 < R(\tau) < 1, \quad \forall \tau \in [0, T).$$

Proof. From system (2.1), we have $\frac{d}{dt}(S(t) + V(t) + I(t) + R(t)) = 0$. This means the total population is constant, that is, $S(t) + V(t) + I(t) + R(t) = 1$ for all $0 < t < T$. Now, we choose an integer $c_0 > 4$ sufficiently large such that $(S(0)V(0), I(0), R(0)) \in [\frac{1}{c_0}, c_0]^4$. In this step for each integer $c > c_0$, we define

$$T_k = \inf\{t \in [0, t) : (S(t), I(t), V(t), R(t)) \notin [\frac{1}{c}, c]^4\},$$

where T_k is stopping time. Hence, by using the idea exposed in [7, 18] the proof become complete. \square

2.2. Equilibria and stability. In this subsection, we investigate the stability of equilibrium points of model (2.2). Since, R dose not appear in three first equation in the model we can reduced our model to the following three dimensional system

$$\begin{aligned} \frac{dS}{dt} &= -\alpha SI - \sigma S, \\ \frac{dV}{dt} &= \sigma S - \vartheta \alpha IV, \\ \frac{dI}{dt} &= \alpha SI + \vartheta \alpha IV - \lambda I. \end{aligned} \tag{2.3}$$

As we mentioned above, we suppose the total population remains constant in time and without loss of generality, that $M = 1$, which results in $E_0 = (0, 1, 0)$. The eigenvalues of the Jacobian of system (2.3) at E_0 are $0, -\sigma$ and $\vartheta \alpha - \lambda$. Therefore, E_0 is stable if $\vartheta \alpha - \lambda < 0$ as σ is positive. Here, one can calculate the basic reproduction number $\mathcal{R}_0 = \frac{\vartheta \alpha}{\lambda}$. Therefore, if $\mathcal{R}_0 < 1$, E_0 is stable, and if $\mathcal{R}_0 > 1$, E_0 is unstable as there is one positive eigenvalue, i.e., $\vartheta \alpha - \lambda > 0$. Hence, system (2.3) has a stable DFE for $\mathcal{R}_0 < 1$ and an unstable one for $\mathcal{R}_0 > 1$.

For some illustration, we investigate trajectories of system (2.2) in the vicinity of equilibrium points. Indeed Specifically, this model has only the disease-free equilibrium point (DFE) $E_0 = (0, 1, 0, 0)$, which is present for any constant total population M . Since the sum of time-derivatives of S, V, I , and R equals zero, we have $S + V + I + R = M$, which implies that the total population remains constant over time. We assume that $M = 1$ without loss of generality. We plot solutions of system (2.2) for $\alpha = 0.7, \sigma = 0.02, \vartheta = 0.9$ and $\lambda = 0.5$ in Fig. 2.

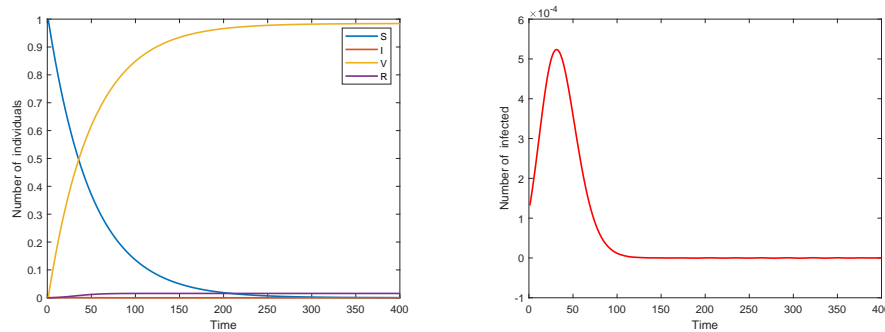


FIGURE 2. Solutions of system (2.2) for $\alpha = 0.7$, $\sigma = 0.02$, $\vartheta = 0.9$ and $\lambda = 0.5$.

3. MATERIALS AND METHODS

In this part of the investigation, the objective is to ascertain the model's parameters to ensure that the simulated data closely mirrors the actual data, followed by utilizing the refined model to assess and forecast the future spread of COVID-19. Within this model framework, population size is held as constant. In other words, we assume that N does not change. We also employed the Runge-Kutta algorithm with the `ode45` command in MATLAB software to solve the model. Furthermore, in order to ensure that the model accurately reflects the actual data and enables precise comparisons and analyses, a time step length of one is utilized to solve the system of differential equations. To solve the system of equations (2.2) using `ode45`, we select the initial condition $(1 - I_0, I_0, 0, 0)$ for each period, where I_0 represents the number of infected people on the first day of the period. As mentioned earlier, each period is characterized by a peak, and since the start of the period is considered the start of the peak, this choice of initial condition is reasonable.

In order to determine the parameters, the genetic algorithm (GA) is employed to minimize the cost function between the model's prediction and the actual data. The cost function, which is based on the mean squared error of the infected data, is formulated accordingly. All simulations were performed using MATLAB R2022a.

3.1. Epidemiological data. The data used in this study was provided by the medical care monitoring center of Yazd Shahid Sadoughi University of Medical Sciences, Yazd, Iran. This data consists of the daily hospitalized cases from Yazd city. The population of the study area is approximately 600,000. We consider all the patients who have PCR tested positive as the infectious category.

3.2. Main results. Epidemic models are commonly used to study the spread of infectious diseases over short periods of time. The behavior of the patient population is often modeled as a Gaussian function, starting from a low value, reaching a maximum value (peak), and then decreasing. However, the behavior of the infected

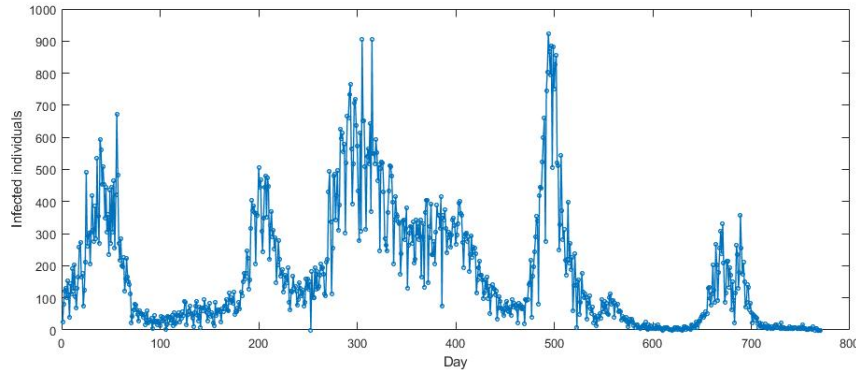


FIGURE 3. Number of daily infected individuals in the Yazd city for 770 days between September 27, 2020 to November 5, 2022.

population during an epidemic may not always follow this pattern. Fig. 3 shows that the behavior of the infected population may have several maximum values, making it difficult to estimate the overall behavior of the epidemic during this time interval with a set of parameter values. This highlights the challenges in mathematically modeling the outbreak and designing policy, especially in the presence of known biases in the data and complexities of the underlying dynamics.

The SVIR model is designed to capture the dynamics of an epidemic, where a susceptible population is infected by infected individuals, recovered individuals gain immunity, and the spread of the disease slows down over time. This aligns with the general trend observed in the graph, where the number of infected individuals initially increases, reaches a peak, and then declines. On the other hand, the SVIR model typically has a unimodal shape, with a single peak representing the epidemic's peak. While the data shows five peaks over the 770-day period. Therefore, the time period can be divided into 5 periods based on the number of disease peaks (or local maximum in Fig. 3).

- The first period is from September 27, 2020, to March 20, 2021, which is 175 days.
- The second period is from March 21, 2021, to June 20, 2021, which is 92 days.
- The third period is from June 21, 2021, to January 8, 2022, which is 202 days.
- The fourth period is from January 9, 2022, to July 12, 2022, which is 185 days.
- The fifth period is from July 13, 2022, to November 5, 2022, which is 116 days.

Moreover, to compare the model estimate of a disease with the real data in a certain period and by considering the total population constant in that period, the data used

are normalized in the range of zero to one. Normalization is a statistical technique used to adjust data to a common scale, which allows fair comparisons between model estimates and actual data, as it takes into account population size and population stability over time. This approach is commonly used in epidemiological studies to quantify disease incidence.

The bootstrap method was employed to calculate the confidence intervals for estimating the four parameters of the SVIR model due to its flexibility and robustness [8]. This non-parametric approach involves repeatedly resampling the data with replacement to create numerous pseudo-datasets, each used to estimate the parameters. By analyzing the distribution of these parameter estimates, we derive empirical confidence intervals that provide insight into the uncertainty of our estimates. The bootstrap method is particularly advantageous in this context because it does not rely on traditional parametric assumptions about the data distribution, which can be unknown or complex. This makes the bootstrap method highly suitable for models like SVIR, where the underlying dynamics can be intricate and the data may not conform to simple distributional forms. The resulting confidence intervals are therefore reliable and reflective of the true variability in the data, enhancing the credibility and accuracy of the parameter estimates for the SVIR model. We calculate the confidence intervals for the model parameters and present them for a period of 5 time intervals.

The Fig. 4 displays a comparison between the number of confirmed cases in Yazd and the SVIR model during the first period, which lasted from September 27, 2020, to March 20, 2021. The blue circles are reported daily data from infected individuals and the solid red line is simulation of the SVIR model. In Fig. 4, we see a huge jump in the number of infected people in Iran. This jump due to the beginning of the fall season and also the beginning of the academic year, followed by the symmetry of another infectious disease such as influenza, was predicted by experts and researchers in advance. But this jump was much more than everyone's imagination and prediction. With the peak of the disease, preventive measures intensified. Then, with the quarantine and the virtualization of educational activities, the number of infected people decreased. The estimated parameters of the SVIR model are $\alpha = 0.73753$, $\sigma = 0.020787$, $\vartheta = 0.76978$ and $\lambda = 0.64097$.

In the first time period the resulting confidence intervals for the parameters are as follows: for α , the 95% confidence interval is [0.23054, 0.8622]; for σ , the confidence interval is [0.0116, 0.417]; for ϑ , the confidence interval is [0.0036, 0.81844]; and for λ , the confidence interval is [0.00043, 0.7182].

The Fig. 5 shows a good estimation of the SVIR model from the infected individuals of the Yazd city from March 21, 2021, to June 20, 2021. The maximum point of this period occurs in April 14, 2021. Considering that people were in quarantine for about 6 months, they were tired of staying at home, and in March 2019, due to the two-week holiday on the occasion of Nowruz, despite health warnings about social distancing, some health and Quarantine was not observed and therefore the

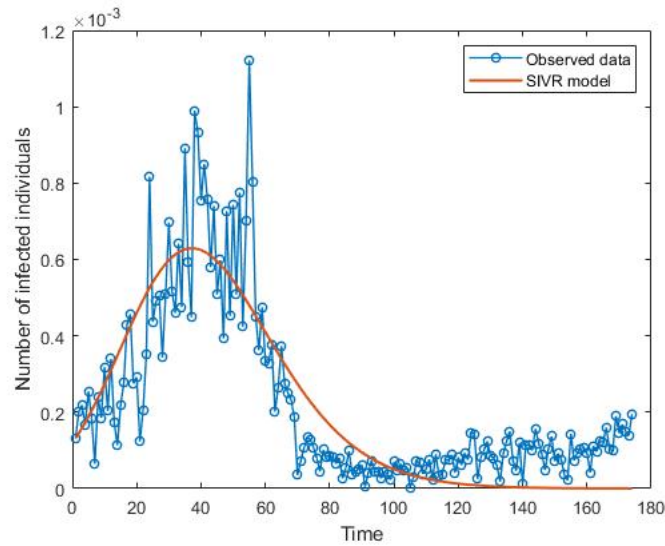


FIGURE 4. Comparison between the number of confirmed cases in Yazd and the SVIR model in the first period from September 27, 2020, to March 20, 2021. The estimated parameters are $\alpha = 0.73753$, $\sigma = 0.020787$, $\vartheta = 0.76978$ and $\lambda = 0.64097$.

number of infected reached its peak again in June 2021. The estimated parameters are $\alpha = 0.30555$, $\sigma = 0.087954$, $\vartheta = 0.11217$ and $\lambda = 0.064819$. In this period, the resulting confidence intervals for the parameters are as follows: for α , the 95% confidence interval is $[0.2405, 0.9829]$; for σ , the confidence interval is $[0.01041, 0.2739]$; for ϑ , the confidence interval is $[0.0136, 0.7727]$; and for λ , the confidence interval is $[0.0324, 0.7764]$. These intervals are reflective of the true variability in the data, thereby enhancing the credibility and accuracy of the parameter estimates for the SVIR model.

In the third period, Yazd experienced a rise in COVID-19 cases around June 21, 2021, coinciding with the start of summer and school closures. Urgent and stricter measures and vaccination may have been implemented to control the situation, leading to a faster decline in infections compared to previous waves. The curve fitting in this period shown in Fig 6. The estimated parameters are $\alpha = 0.80263$, $\sigma = 0.25389$, $\vartheta = 0.48436$ and $\lambda = 0.388$. The resulting confidence intervals for the parameters are as follows: for α , the 95% confidence interval is $[0.3378, 0.9896]$; for σ , the confidence interval is $[0.1033, 0.4188]$; for ϑ , the confidence interval is $[0.0693, 0.7242]$; and for λ , the confidence interval is $[0.0426, 0.6235]$.

The estimated parameters for the 4th period are as follows: $\alpha = 0.99985$, $\sigma = 0.038443$, $\vartheta = 0.48121$, and $\lambda = 0.66579$. The 95% confidence intervals for these

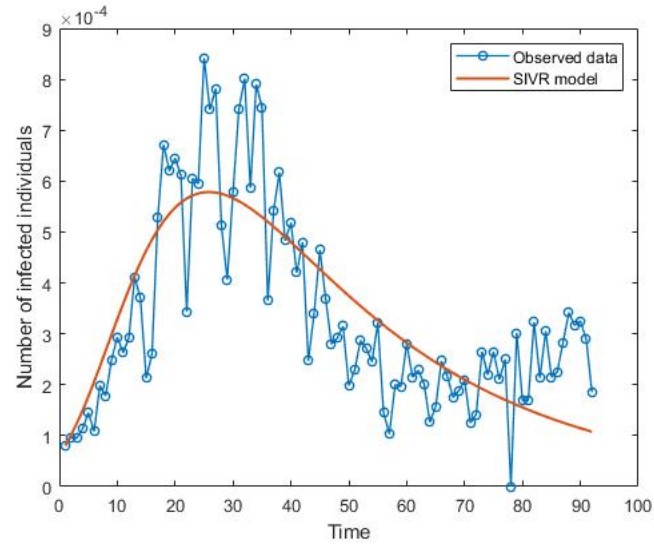


FIGURE 5. Comparison between the number of confirmed cases in Yazd and the SVIR model in the second period from June 21, 2021, to January 8, 2022. The estimated parameters are $\alpha = 0.30555$, $\sigma = 0.087954$, $\vartheta = 0.11217$ and $\lambda = 0.064819$.

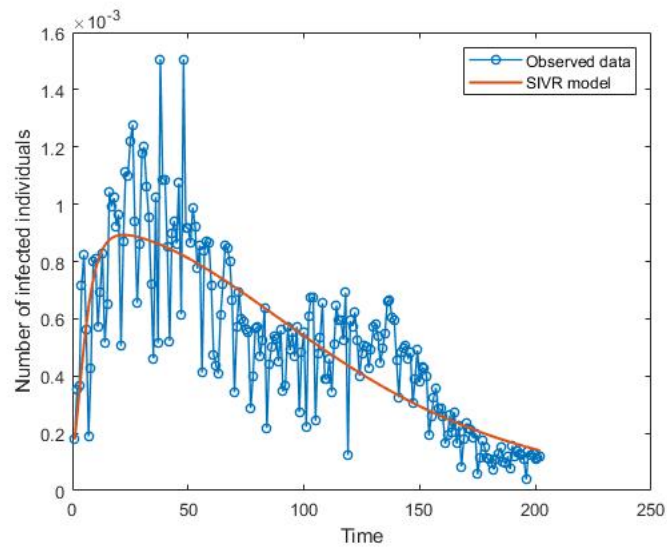


FIGURE 6. Comparison between the number of confirmed cases in Yazd and the SVIR model in the third period from June 21, 2021, to January 8, 2022. The estimated parameters are $\alpha = 0.80263$, $\sigma = 0.25389$, $\vartheta = 0.48436$ and $\lambda = 0.388$.

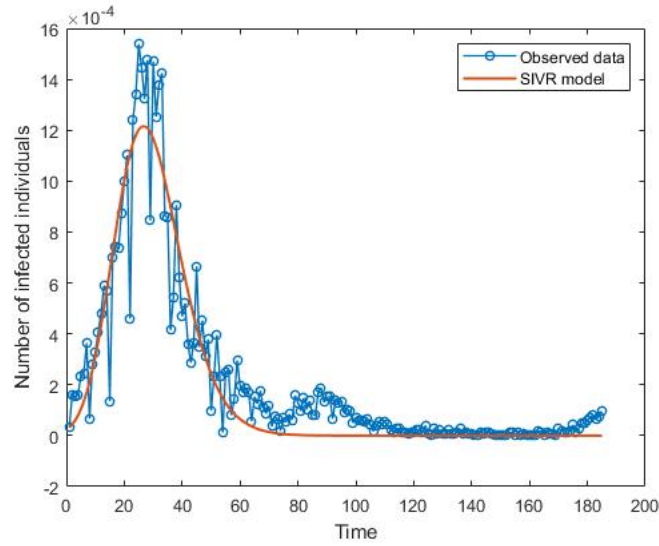


FIGURE 7. Comparison between the number of confirmed cases in Yazd and the SVIR model in the fourth period from January 9, 2022, to July 12, 2022. The estimated parameters are $\alpha = 0.99985$, $\sigma = 0.038443$, $\vartheta = 0.48121$ and $\lambda = 0.66579$.

parameters are:

$$\alpha : [0.2845, 1.0001], \quad \sigma : [0.0103, 0.1280],$$

$$\vartheta : [0.2210, 0.7158], \quad \lambda : [0.3717, 0.7545].$$

The estimated parameters for the 5th period are as follows: $\alpha = 0.31935$, $\sigma = 0.082176$, $\vartheta = 0.12697$, and $\lambda = 0.10583$. The 95% confidence intervals for these parameters are:

$$\alpha : [0.3057, 0.9251], \quad \sigma : [0.0261, 0.1976],$$

$$\vartheta : [0.0777, 0.6604], \quad \lambda : [0.0883, 0.6895].$$

In the fourth and fifth periods (see Figures 7 and 8), there is a peak on the 20th day from the start of the period, followed by a decrease in the number of patients, eventually approaching zero. Figures 4 to 8 clearly demonstrate that the SVIR model aligns closely with the data. Additionally, we infer that if we select the starting point of the model where the number of infected individuals is initially increasing within the period, this model effectively captures the behavior and dynamics of the infected population.

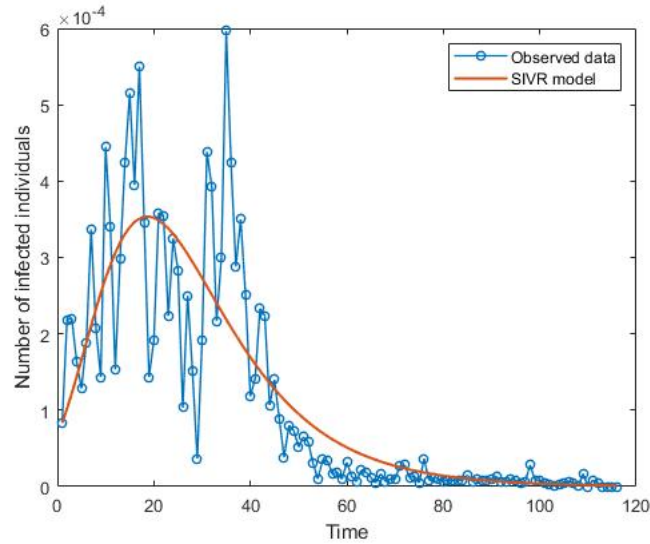


FIGURE 8. Comparison between the number of confirmed cases in Yazd and the SVIR model in the fifth period from July 13, 2022, to November 5, 2022, The estimated parameters are $\alpha = 0.31935$, $\sigma = 0.082176$, $\vartheta = 0.12697$ and $\lambda = 0.10583$.

4. CONCLUSION

The SVIR is a relatively simple model with a clear interpretation. Each compartment (Susceptible, Infected, Vaccinated, Recovered) represents a well-defined stage of the disease. This simplicity allows researchers to understand how changing parameters (e.g., transmission rate) affects the spread of the disease. Under certain assumptions, SVIR can be used to predict the future course of an outbreak, helping with public health planning and resource allocation. From mathematical view point, the SVIR model assumes a homogenous population with constant transmission rates. These assumptions may not hold true for the entire 770 days, especially if there were significant changes in population behavior or the virus itself. On the other hands, the SVIR model typically has a unimodal shape, with a single peak representing the epidemic's peak. While the data shows five peaks over the 770-day period. Therefore, the time period can be divided into 5 periods based on the number of disease peaks. In each period we estimate parameters of the model and fit the solution of SVIR model with the data. The figures show that the model fits the data well in each period.

To the best of our knowledge, papers that apply mathematical models to COVID-19 data typically focus on short time, estimating model parameters for small durations. Thus far, the SVIR model has not been utilized with any dataset. The

concept of segmenting an extended timeframe into smaller intervals, spanning approximately 300 days, grounded in the SIR model, has only been validated in [22], albeit with fewer peaks. Despite numerous constraints and a considerable number of model parameters, we successfully aligned the data with the model. It should be noted, the accuracy of the model will depend on the quality of the data on infected individuals. Reporting inconsistencies or missing data can affect the fitted model.

It is noteworthy that, according to the parameter estimates of the model, during a distinct period characterized by a single peak, the onset of the upward trend in case numbers marks the beginning of the period of interest. Consequently, a reliable estimation of the peak value becomes attainable. This facilitates the implementation of suitable public health interventions aimed at curbing the spread of the disease.

While our current work offers valuable insights using ordinary differential equations, we recognize the advantages of fractional order models in capturing memory effects and complex dynamics observed in real-world epidemic data. Therefore, future research will extend our model to incorporate fractional calculus, enhancing its flexibility and precision. This approach aims to provide a deeper understanding of the temporal dynamics and long-term behavior of the epidemic, contributing to both theoretical advancements and practical public health strategies for managing COVID-19 and similar infectious diseases.

ETHICS STATEMENTS

This study has been approved by the ethics committee of SSU (Registration code: IR.SSU.REC.1401.063). Data records were anonymous, so informed consent was waived.

ACKNOWLEDGEMENTS

The authors want to acknowledge the staff of infectious diseases research center of Shahid Sadoughi University of Medical Sciences of Yazd.

REFERENCES

- [1] M. Abdi. Coronavirus disease 2019 (COVID-19) outbreak in iran: Actions and problems. *Infection Control & Hospital Epidemiology*, **41**(6)(2020), 754–755.
- [2] M. Abdi and R. Mirzaei. Iran without mandatory quarantine and with social distancing strategy against coronavirus disease (COVID-19). *Health security*, **18**(3)(2020), 257–259.
- [3] M. H. Akrami. Analysis of a fractional siqr model with caputo-fabrizio derivative. *Caspian Journal of Mathematical Sciences (CJMS)*, **12**(2)(2023), 397–413.
- [4] C. G. Antonopoulos, M. H. Akrami, V. Basios, and A. Latifi. A generic model for pandemics in networks of communities and the role of vaccination. *Chaos: An Interdisciplinary Journal of Nonlinear Science*, **32**(6)(2022), 063127.
- [5] S. Anupong, T. Chantanasaro, C. Wilasang, N. C. Jitsuk, C. Sararat, K. Sornbundit, B. Pattanasiri, D. L. Wannigama, M. Amarasiri, S. Chadsuthi, and C. Modchang. Modeling vaccination strategies with limited early covid-19 vaccine access in low- and middle-income countries: A case study of thailand. *Infectious Disease Modelling*, **8**(4)(2023), 1177–1189.

- [6] I. Cooper, A. Mondal, and C. G. Antonopoulos. A SIR model assumption for the spread of COVID-19 in different communities. *Chaos, Solitons & Fractals*, **139**(2020), 110057.
- [7] N. Dalal, D. Greenhalgh, and X. Mao. A stochastic model of aids and condom use. *Journal of Mathematical Analysis and Applications*, **325**(1)(2007), 36–53.
- [8] F. M. Dekking, C. Kraaikamp, H. P. Lopuhaä, and L. E. Meester. *A Modern Introduction to Probability and Statistics: Understanding why and how*. Springer Science & Business Media, 2006.
- [9] M. Kazempour Dizaji, M. Varahram, R. Roozbahani, A. Abedini, A. Zare, A. Kiani, M. A. Emamhadi, N. Alizadeh Kolahdozi, S. A. Nadji, and M. Marjani. Simulation of COVID-19 disease epidemic in Iran based on SIR model. *Health Science Monitor*, **1**(1)(2022), 1–9.
- [10] F. Madadzadeh, S. Y. Ghelmani, and T. F. Tafti. Spatial analysis of the COVID-19 prevalence pattern in yazd province, central part of Iran (february 2020 to january 2021). *Journal of Community Health Research*, (2022).
- [11] A. Malik, N. Kumar, and K. Alam. Estimation of parameter of fractional order COVID-19 SIQR epidemic model. *Materials Today: Proceedings*, **49**(2022), 3265–3269.
- [12] D. K. Mamo. Model the transmission dynamics of covid-19 propagation with public health intervention. *Results in Applied Mathematics*, **7**(2020), 100123.
- [13] S. Moein, N. Nickaeen, A. Roointan, N. Borhani, Z. Heidary, S. H. Javanmard, J. Ghaisari, and Y. Gheisari. Inefficiency of sir models in forecasting covid-19 epidemic: a case study of isfahan. *Scientific reports*, **11**(1)(2021), 4725.
- [14] S. F. Mousavi. Psychological well-being, marital satisfaction, and parental burnout in iranian parents: The effect of home quarantine during COVID-19 outbreaks. *Frontiers in Psychology*, **11**(2020).
- [15] P. Shahrear, S. M. S. Rahman, and M. M. H. Nahid. Prediction and mathematical analysis of the outbreak of coronavirus (covid-19) in bangladesh. *Results in Applied Mathematics*, **10**(2021), 100145.
- [16] L. F. Shampine and M. W. Reichelt. The matlab ode suite. *SIAM journal on scientific computing*, **18**(1)(1997), 1–22.
- [17] A. Tiwari. Modelling and analysis of COVID-19 epidemic in India. *Journal of Safety Science and Resilience*, **1**(2)(2020), 135–140.
- [18] E. Tornatore, P. Vetro, and S. M. Buccellato. SIVR epidemic model with stochastic perturbation. *Neural Comput. & Applic.*, **24**(2014), 309–315.
- [19] <https://covid19.who.int/>. WHO coronavirus (COVID-19) dashboard. *World Health Organization*, (2020).
- [20] <https://www.who.int/emergencies/diseases/novel-coronavirus-2019>. Coronavirus disease (COVID-19) outbreak. *World Health Organization*, (2019).
- [21] F. Wu, S. Zhaio, B. Yu, Y.-M. Chen, W. Wang, Z.-G. Song, Y. Hu, Z.-W. Tao, J.-H. Tian, P. Yuan-Yuan, M.-L. Yuan, Y.-L. Zhang, F.-H. Dai, Y. Liu, Q.-M. Wang, J.-J. Zheng, L. Xu, E. C. Holmes, and Y.-Z. Zhang. A new coronavirus associated with human respiratory disease in China. *Nature*, **579**(7798)(2020), 265.
- [22] Z. Zare and N. Vasegh. Modeling and analysis of the spread of the COVID-19 pandemic using the classical SIR model. *Journal of Control*, **14**(5)(2021), 89–96.